Chapter 9
Dark Matter

The fact that a significant fraction of the matter in the contemporary Universe cannot be inside stars was already noted by Fritz Zwicky in 1933. Using the virial theorem, Zwicky estimated the total mass of the Coma cluster from the motion of some of its galaxies. He measured a mass much higher than that obtained from the brightness of the galaxies. Subsequent studies of galaxies and galaxy clusters confirmed that the main contribution to their masses was done by some invisible matter. This was the first indication that most of the matter in the Universe was not in the form of ordinary baryonic matter. However, at that time the cosmological fraction of the energy density of matter, Ω_m, was very poorly known.

Now we know that the BBN data fix the present day fraction of the baryon energy density at the level of $\Omega_B \approx 0.05$, see Chap. 8, while the total energy density of non-relativistic matter is approximately five times larger, $\Omega_m \approx 0.3$, as it is found from the analysis of the large scale structure of the Universe and the angular fluctuations of the CMB. These data provide very strong support to the idea that most of the matter in the Universe is not the usual baryonic one.

At the beginning of the 1990s, it was believed that $\Omega_{tot} < 1$ and that the Universe was open, in contradiction with the inflationary prediction of a 3D flat universe. There were even attempts to modify the inflationary scenario in such a way that it could naturally lead to $\Omega_{tot} < 1$, but they were not particularly successful. On the other hand, there was an accumulation of data indicating the inconsistencies of the open universe model with low Ω_{tot}. In particular, the calculated Universe age in such models was smaller than the estimates obtained by the nuclear chronology and by the ages of old stellar clusters. All such problems were eliminated after the discovery of the accelerating expansion of the Universe. Now it is established that the Universe is practically flat with $\Omega_{tot} = 1$, where the necessary 0.7 comes from the contribution of a quite mysterious form of energy, currently called dark energy.

More details on this topic can be found in Bergstrom (2000), which provides an extended review on the observational evidence of dark matter and possible detection methods.

C. Bambi and A.D. Dolgov, *Introduction to Particle Cosmology*,
UNITEXT for Physics, DOI 10.1007/978-3-662-48078-6_9

9.1 Observational Evidence

The amount of matter in a galaxy can be inferred from the study of the rotational velocity curve of the gas clouds around the galaxy. The velocity v as a function of the radial distance from the galactic center r can be measured from the Doppler shift of spectral lines. In Newtonian mechanics, we have

$$\frac{v(r)^2}{r} = \frac{G_{\rm N} M(r)}{r^2} \Rightarrow v(r) = \sqrt{\frac{G_{\rm N} M(r)}{r}}\,, \tag{9.1}$$

where $M(r)$ is the total mass within the radius r. If the stars provided the main contribution to the mass of a galaxy, at large radii, beyond the visible galaxy, one should expect $v \sim r^{-1/2}$. However, this is not what we observe: at large radii $v \sim const$, which implies $M(r) \sim r$, namely a galaxy extends to larger radii with respect to that is seen by optical observations.

Systematic and accurate measurements of galactic rotation curves started in the 1970s (Freeman 1970) with spiral galaxies. Spiral galaxies are a class of galaxies consisting of a central bulge and a thin disk. In the case of spiral galaxies, we find that v increases linearly at small radii until it reaches a typical value of about 200 km/s, and then it remains constant. On the contrary, the surface luminosity of the disk falls off exponentially. Today we know the rotational curves of thousands of galaxies. The measurements suggest the existence of a dark matter halo surrounding every galaxy and with the mass about ten times larger than the mass of the visible stars in the disk. It is worth noting that other types of galaxies seem also to be dark matter dominated with even larger fraction of dark matter. For instance, this is the case of dwarf spiral galaxies. Their rotational curve continues rising well beyond the radius of the luminous disk. Figure 9.1 shows the rotational curve of the galaxy M33, which belongs to the Local Group. v does not reach a constant value but continues rising. The dark matter contribution to the total galaxy mass is higher than in the case of normal spiral galaxies. Strictly speaking, these methods only measure local density inhomogeneities. Moreover, the observational identification of the dark matter halo is difficult. Eventually, an estimate of the cosmological fraction of the matter density suggests $\Omega_m \approx 0.2 - 0.4$. The study of virial velocities in galaxy clusters demonstrates the same features and provides similar results.

The measurement of Ω_m inferred from the study of galactic rotation curves is supported by a combination of independent results. The study of the supernovae Ia at high redshift provides the strongest evidence for the present accelerating expansion of the Universe. If we assume that the Universe is only made of non-relativistic matter and with a non-vanishing cosmological constant, these data can be used to constrain the allowed area on the $(\Omega_\Lambda, \Omega_m)$ plane. The analysis of the CMB anisotropies leads to the conclusion that the Universe is almost flat, namely $\Omega_\Lambda + \Omega_m \approx 1$. The combination of supernovae and CMB data leads to $\Omega_m \approx 0.30$.

All the above methods can provide an estimate of the total gravitating matter in the Universe. They do not really tell us anything about its nature. The stellar

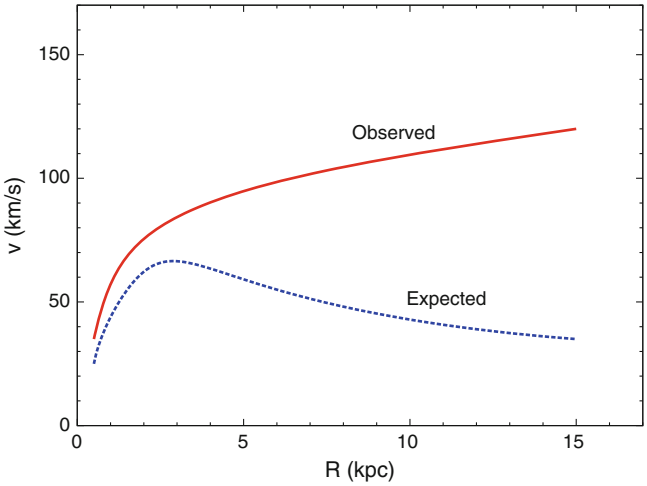

Fig. 9.1 Sketch of the observed HI rotation *curve* of the dwarf galaxy M33 (*red solid line*) and of that expected from the stellar distribution (*blue dashed line*)

contribution is $\Omega_{stars} \sim 0.003 - 0.01$, which is thus a small fraction of Ω_m. A much larger contribution to the mass can be made by the gas in the interstellar medium or non-luminous bodies like planets. As shown in Chap. 8, the study of the primordial abundances of light elements requires that the fraction of baryons is $\Omega_B \approx 0.05$ while any other form of gravitating matter does not make any contribution into it.

While there are scenarios in which only a fraction of the total amount of baryons were available for the nucleosynthesis in the early Universe, they definitively require exotic mechanisms. The most natural interpretation is that most of the dark matter is not made of baryons. Non-baryonic dark matter is also required to explain the formation of large scale structures (see Chap. 12). The combination of measurements of the CMB temperature fluctuations, which probe very large scales, and measurements of the galaxy power spectrum, which probe smaller scales, proves that non-baryonic matter is necessary to explain observational data, because baryons were locked in with photons until recombination, which prevented a quick growth of fluctuations.

The most convincing evidence for the existence of non-baryonic dark matter probably comes from the Bullet Cluster (Clowe et al. 2004). This is a system consisting of a subcluster that passed through a cluster about 150 Myr ago. The key-point is that the collision between the two clusters seems to have caused a separation of the dark matter component from the baryonic one. Observations show that stars, baryonic matter in the form of gas, and dark matter have different collision properties and seem to rule out the possibility of explaining dark matter as a modification of gravity at kpc scale. Using optical observations, we can study the distributions of the stars, which are not strongly affected by the cluster collision. X-ray measurements track the distribution of the hot gas, which represents the main component of the baryonic matter. Because of electromagnetic interactions among the particles of the

gas, the cluster collision made the baryonic matter concentrate at the center of the system. Lastly, gravitational lensing studies map the distribution of gravitating matter. Observations show that most of the mass in the cluster was not affected by the collision. The interpretation of these observations is that most of the mass consists of weakly interacting dark matter and, unlike the galaxy curves, it is independent of possible modifications of Newton's law at kpc scales. We note that in the past there was a controversial issue concerning the initial infall velocity of the clusters, which seemed to be beyond that expected within the Standard Cosmological Model. If so, a modification of gravity might have been necessary. However, this tension seems to be solved by more recent studies (Lage and Farrar 2015).

9.2 Dark Matter Candidates

After it was realized that most matter in the Universe is not luminous, astronomical observations focused on the search for objects such as black holes, neutron stars, faint old white dwarfs, planets, and similar bodies, collectively called massive astrophysical compact halo objects (MACHOs). In the 1970s, the BBN studies pointed out the discrepancy between baryonic matter, $\Omega_B \approx 0.05$, and gravitating matter inferred by dynamical methods, $\Omega_m \approx 0.2 - 0.4$. While there could be scenarios in which only a small fraction of the total baryons in the Universe were available at the BBN, they definitively require quite exotic mechanisms. Astronomical surveys for gravitational microlensing attempting to find MACHOs (Afonso 2003; Alcock 2000; Tisserand 2007) have succeeded in the discovery of such objects with masses of the order of the Solar mass, but their amount is very small, and definitively too small to make all the necessary invisible matter. The current data on the abundance of MACHOs in the Galactic Halo are shown in Fig. 9.2.

Dark matter candidates can be grouped into three classes, namely cold dark matter (CDM), warm dark matter (WDM), and hot dark matter (HDM). The key-point to belong to one or another group is the distance that the particle travelled during the Universe history. By definition, CDM particles have the free-streaming length much shorter than the typical size of a protogalaxy. WDM candidates have the free-streaming length of the order the typical size of a protogalaxy, while in the HDM case the free-streaming length is much larger than the size of a protogalaxy. The particles' free-streaming length is a crucial parameter in structure formation theory, because primordial density fluctuations with wave length shorter than the free-streaming length are washed out by the particle motion from the overdense regions to the underdense ones.

The free-streaming length of dark matter particles that were in thermal equilibrium in the early Universe is determined by the ratio of their decoupling temperature to their mass, T_f/m. The process of decoupling (or freezing) is described in Chap. 5. For example, neutrinos decoupled at $T_f \sim 1$ MeV, so the length of their travel in the FRW background till they became non-relativistic is equal to

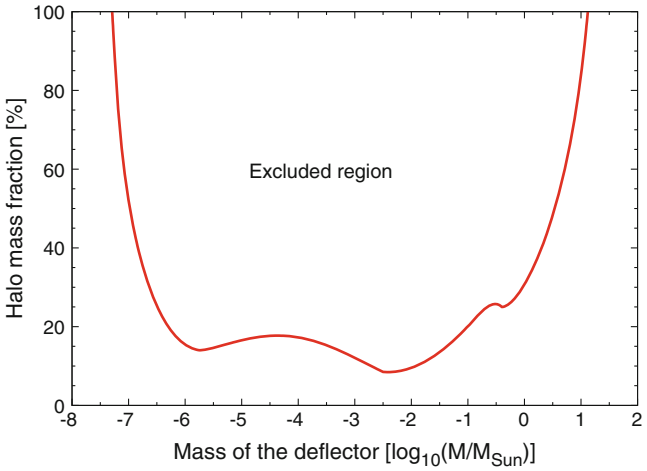

Fig. 9.2 Sketch of the constraints on the halo mass fraction of MACHOs as a function of the MACHO mass

$$\ell_{fs} = a(t) \int_{t_f}^{t_{fs}} \frac{dt'}{a(t')} + (\text{nonrel}) \approx 2t_{fs}\,, \tag{9.2}$$

where the second term is the length of the neutrino propagation after it became non-relativistic, which is small and can be neglected. It is assumed that the cosmological expansion regime is relativistic with $a(t) \sim \sqrt{t}$. The upper limit of the integration is taken at the moment when neutrinos became non-relativistic, i.e., their temperature dropped down e.g., to $m_\nu/3$.

The mass inside the free streaming radius can be estimated as

$$M_{fs} = \frac{32\pi}{3}\,\rho t_{fs}^3 = M_{\rm Pl}^2 t_{fs}\,, \tag{9.3}$$

where we took for ρ the radiation dominated stage expression $\rho = 3M_{\rm Pl}^2/(32\pi t^2)$. The free streaming time can be roughly estimated as $t_{fs} \sim 0.1 M_{\rm Pl}/T^2 \approx M_{\rm Pl}/m_\nu^2$. see Eq. (5.14). Thus finally we obtain for particles (not necessarily neutrinos) that were relativistic at decoupling

$$M_{fs} \sim \frac{M_{\rm Pl}^3}{m_\nu^2} \approx 10^{18} M_\odot \left(\frac{\rm eV}{m}\right)^2\,. \tag{9.4}$$

Evidently, for neutrinos with $m_\nu < 1$ eV, the free streaming mass is much larger than the galactic mass. So neutrinos for sure make HDM. Particles with $m \sim 1$ keV would make WDM, while heavier ones would form CDM.

On the other hand, models with dark matter particles produced in non-thermal processes are also possible and an example of that is the axion, which is briefly

presented in Sect. 9.2.2. Despite a very small mass, axions form CDM because they were created at rest.

CDM, WDM, and HDM predict different scenarios for the large scale structure formation in the Universe, namely for the formation of galaxies, galaxy clusters, and superclusters. In the case of CDM, smaller structures are formed first and then they congregate to form larger structures. In the case of HDM, density fluctuations at small scales are washed out and therefore the first structures are large. The latter must then fragment into galaxies. Observations favor CDM candidates, because looking at high redshift we see that galaxies formed first, while clusters and superclusters formed later. There is recent accumulated evidence in favor of some fraction of WDM as well.

An interesting class of dark matter candidates are the so-called weakly interacting massive particles (WIMPs). All these candidates interact through the weak nuclear force or through a force with a similar strength. They weakly interact with ordinary matter, but not too weakly to make a direct detection impossible. Moreover, they may have a mass in the GeV or TeV range, which makes also their number density around us not too low for a direct detection. Such dark matter candidates may be produced in particle physics colliders, because their mass is not too high. Lastly, they are an appealing class of candidates even because of the so-called "WIMP miracle". If we consider particles with a mass of order 100 GeV$-$1 TeV subject to the weak nuclear force in the primordial plasma, we see that they should have decoupled at a temperature of order 10 GeV. Interestingly, their abundance today would be consistent with $\Omega_m \sim 0.3$, which is the value requested by observations.

9.2.1 Lightest Supersymmetric Particle

As discussed in Sect. 3.4.1, Supersymmetry is mainly motivated by the hierarchy problem, namely the necessity to protect the Higgs mass from quantum corrections that would make it huge. Supersymmetric models have the appealing feature of having potentially good dark matter candidates.

In the minimal supersymmetric extension of the Standard Model of particle physics, the Lagrangian of the theory admits dangerous terms that would predict the non-conservation of the baryon and lepton numbers. For instance, these terms would make proton unstable, in disagreement with the experimental constraints. The problem can be fixed by imposing a new symmetry called R-parity. With such a symmetry, the lightest supersymmetric particle, or LSP, is stable. If the LSP is electrically neutral, it would be a good dark matter candidate. In many supersymmetric models, the LSP is the lightest neutralino, which is a superposition of the bino, i.e., the fermionic super-partner of the Standard Model gauge boson associated with the $U_Y(1)$ field, the neutral wino, i.e., the fermionic super-partner of the electrically-neutral Standard Model gauge boson associated with the $SU_L(2)$ field, and the neutral higgsinos, i.e., the fermionic super-partners of the supersymmetric Higgs scalars. The

lightest neutralino is often considered one of the best dark matter candidates, even though supersymmetric particles at LHC have not been so far discovered.

In other models, the LSP dark matter candidate may be the axino, fermionic super-partner of the axion, or the gravitino, spin-3/2 super-partner of the graviton in Supergravity models where gravity is also taken into account and supersymmetrized. The lightest sneutrino (the scalar super-partner of the Standard Model neutrinos) is not a good dark matter candidate in the minimal supersymmetric extension of the Standard Model, because of its large cross section with nucleons, which is today experimentally excluded. However, sneutrinos can still be good dark matter candidates in more sophisticated models.

9.2.2 Axion

As briefly mentioned in Sect. 3.4.4, the strong CP problem in QCD may be solved with the introduction of a new global $U(1)$ symmetry, which is spontaneously broken at low energies, about 100 MeV. The theory predicts the existence of a spin-0 particle called axion, which gets a non-vanishing mass after the formation of the vacuum condensate of gluon fields at the QCD phase transition. Above this phase transition, axions would be massless Goldstone bosons, see Sect. 7.3.5 for some explanation, but below it an explicit symmetry breaking is induced by the condensate and axions acquire a small mass due to non-perturbative QCD effects:

$$m_a \approx 0.62 \left(\frac{10^7 \text{ GeV}}{f_a} \right) \text{ eV} , \tag{9.5}$$

where f_a is the $U(1)$ symmetry breaking scale. Constraints on the axion mass come from direct laboratory search and astrophysical observations (stellar cooling and supernova dynamics) (Raffelt 1997). Axions with a mass at the level of a few μeV might still be viable dark matter candidates. Despite such a low mass, they would be CDM particles, because they would have been produced at rest and never been in thermal equilibrium.

9.2.3 Super-Heavy Particles

In the Standard Model of particle physics, fermions, quarks, and some gauge bosons get a mass after the electroweak symmetry breaking. The masses generated in this way should be of the order of the electroweak symmetry breaking scale, which is about a few hundred GeV, multiplied by the coupling constants of their interaction with the Higgs boson. In particular, that is how the masses of the intermediate bosons $\sim$100 GeV are generated. In the same way, the GUT scenarios naturally predict

super-heavy gauge or Higgs-like bosons with masses of the order of the GUT scale $M_{\rm GUT} \sim 10^{14} - 10^{16}$ GeV. In principle there could be other super-heavy particles, which happen to be stable or very much long-lived due to some (quasi) conserved quantum number. If these particles do not have long range electromagnetic and strong interactions, they could be good dark matter candidates. Their direct and indirect detections may be extremely difficult, if not impossible, since their large mass implies a very low cosmological number density. Moreover, it is not clear if so heavy particles can be stable against gravitational decay. While we do not have any reliable quantum gravity theory to describe particle processes at the Planck scale, from heuristic arguments we may expect the possibility of a decay via a virtual black hole (Bambi et al. 2007) with the lifetime

$$\tau \sim \frac{M_{\rm Pl}^4}{M_{\rm GUT}^5} \sim 10^{-13}\ {\rm s}\,, \tag{9.6}$$

see the discussion at the end of Sect. 7.3.4. The decay may be forbidden by some unknown symmetry, but broken symmetries or global symmetries cannot do it, which makes difficult to have these particles stable.

9.2.4 Primordial Black Holes

Primordial black holes have been considered for a long time as viable dark matter candidates. They may have been produced in the early Universe, well before the advent of the first stars, from the collapse of overdense regions, gravitational collapse of cosmic strings or domain walls, during first or second order phase transitions, etc. For a review, see e.g., Carr (2003). In most scenarios, relative energy perturbations of order unity stopped expanding and recollapsed as soon as they crossed the cosmological horizon. In this case, the maximum mass of primordial black holes is set by the total mass within the cosmological horizon, namely $M_{\rm hor} = M_{\rm Pl}^3/E^2$ where E is the energy scale at which primordial black holes formed, and it turns out to be

$$M_{BH} \approx M_{\rm Pl}^2\, t_{\rm f} \approx 5 \cdot 10^{26} \frac{1}{\sqrt{g_*}} \left(\frac{1\ {\rm TeV}}{T_{\rm f}}\right)^2\ {\rm g}\,, \tag{9.7}$$

where g_* is the effective number of relativistic degrees of freedom at the time $t_{\rm f}$ of the formation of primordial black holes, when the temperature of the Universe was $T_{\rm f}$. In this way, M_{BH} may range from the Planck mass $M_{\rm Pl}$, for black holes formed at the Planck epoch, to $M_\odot$, for black holes formed at the QCD phase transition. Primordial black holes formed after the QCD phase transition may have much larger masses, as it is argued in Sect. 7.4, Eq. (7.62).

Low mass black holes are extremely compact objects. For example, a black hole with the mass $M_{BH} = 10^{15}$ g has the radius $r_g \approx 10^{-13}$ cm. Because of that,

they behave as super-heavy particles possessing only gravitational interactions. This makes their possible detection very difficult.

However, this is true only in the limit of classical physics. At semiclassical level, black holes are not really black and stable, but emit thermal radiation with the equilibrium black body spectrum[1] and temperature $T_{BH} = M_{\rm Pl}^2/8\pi M_{BH}$, see Eq. (7.24). This expression for the temperature is true for a non-rotating and electrically neutral black hole. This process is called the Hawking radiation. The evaporation timescale is $\tau_{\rm evap} \sim M_{BH}^3/M_{\rm Pl}^4$; more accurate expression is given by Eq. (7.26). Primordial black holes with the initial mass $M_{BH} \sim 5 \cdot 10^{14}$ g would have the lifetime of the order of the Universe age. Primordial black holes with larger masses could survive to our time and may be registered by their Hawking radiation. However, the black hole temperature quickly decreases with the black hole mass and the Hawking emission for macroscopic black holes become completely negligible.

While primordial black holes may still represent a fraction of dark matter, their cosmological abundance is strongly constrained. Primordial black holes with an initial mass $M_{BH} \lesssim 5 \cdot 10^{14}$ g would have already evaporated ($\tau_{\rm evap}$ is shorter than the age of the Universe). However, it is possible that quantum gravity effects make Planck mass black holes stable (Adler et al. 2001), and in this case they may form the whole dark matter in the Universe. For $M_{BH} \sim 10^{15} - 10^{16}$ g, there is a strong bound on their possible abundance, at the level of $\Omega_{BH} \lesssim 10^{-8}$ (Page and Hawking 1976), derived from the observed intensity of the diffuse γ-ray background. So they may contribute only a tiny fraction of the non-relativistic matter in the Universe. The abundance of primordial black holes in the mass range $10^{17} - 10^{26}$ g might be constrained from the observations of old neutron stars in regions in which the density of dark matter is supposed to be high (Pani and Loeb 2014). For higher mass, $M_{BH} \gtrsim 10^{26}$ g, the most stringent constraints come from the search for MACHOs (Afonso 2003; Alcock 2000; Tisserand 2007).

9.3 Direct Search for Dark Matter Particles

Direct detection experiments look for signals from the passage of dark matter particles through specially designed very sensitive detectors. Most of these experiments are aimed at the detection of WIMPs scattering off nuclei of the detector. They typically operate in deep underground laboratories to reduce the cosmic ray background. A partial list of past, present, and future direct detection experiments is presented in Table 9.1. For a recent overview on the status of direct searches for dark matter, see e.g., Schumann (2015).

The interaction rate of WIMPs with a detector mainly depends on their masses and cross section. For this reason, the results of experiments are commonly expressed

[1] In fact the spectrum is not really black but is distorted by the effects of the particle propagation in the gravitational field of the black hole after the emission from the horizon. For more detail see Sect. 7.3.4.

Table 9.1 Partial list of direct detection experiments

Experiment	Target	Location
ADMX	Axion	University of Washington (Washington)
CDMS	WIMPs	Soudan Underground Laboratory (Minnesota)
CoGeNT	WIMPs	Soudan Underground Laboratory (Minnesota)
COUPP	WIMPs	Fermilab (Illinois)
CRESST	WIMPs	Gran Sasso National Laboratory (Italy)
DAMA	WIMPs	Gran Sasso National Laboratory (Italy)
DarkSide	WIMPs	Gran Sasso National Laboratory (Italy)
DEAP	WIMPs	SNOLAB (Canada)
DRIFT	WIMPs	Boulby Underground Laboratory (UK)
EDELWEISS	WIMPs	Modane Underground Laboratory (France)
EURECA	WIMPs	Modane Underground Laboratory (France)
LUX	WIMPs	Sanford Underground Laboratory (South Dakota)
PICASSO	WIMPs	SNOLAB (Canada)
PVLAS	Axion	Legnaro National Laboratory (Italy)
SIMPLE	WIMPs	Laboratoire Souterrain à Bas Bruit (France)
WARP	WIMPs	Gran Sasso National Laboratory (Italy)
XENON	WIMPs	Gran Sasso National Laboratory (Italy)
ZEPLIN	WIMPs	Boulby Underground Laboratory (UK)

as constraints in the WIMP mass-cross section plane. The WIMP interaction rate is $\Gamma = nv\sigma$, where n is the WIMP number density, v is the WIMP velocity, and σ is the cross section of WIMP scattering off nucleus. The local dark matter energy density is estimated to be $\rho \approx 0.4$ GeV/cm^3 and therefore $n = \rho/m$ depends on the unknown WIMP mass m. The WIMP velocity distribution is usually assumed to be of Maxwellian form with the mean velocity close to the velocity of the stars in the Galaxy, namely around 200 km/s in the Solar System. Cross sections can be grouped into two classes, spin-independent and spin-dependent cross sections. Theoretically motivated scenarios usually have WIMPs with spin-independent cross sections, but generally speaking models with spin-dependent cross sections cannot be excluded.

A possible observational signature of dark matter is an annual modulation of the signal due to the variation of the relative velocity of Earth and WIMPs. The Solar System moves with a velocity of about 220 km/s with respect to the Galactic rest-frame and the motion of the Earth around the Sun is along the same direction in June and in the opposite direction in December. As a result, we should expect the variation of the WIMP scattering rate by about 3 %, with the maximum rate in June and the minimum rate in December. The daily rotation of Earth may cause a daily forward/backward asymmetry of the nuclear recoil direction, which can also be used as an experimental signature. Another interesting signature would be the measurement of the propagation direction of the colliding particles. In this case,

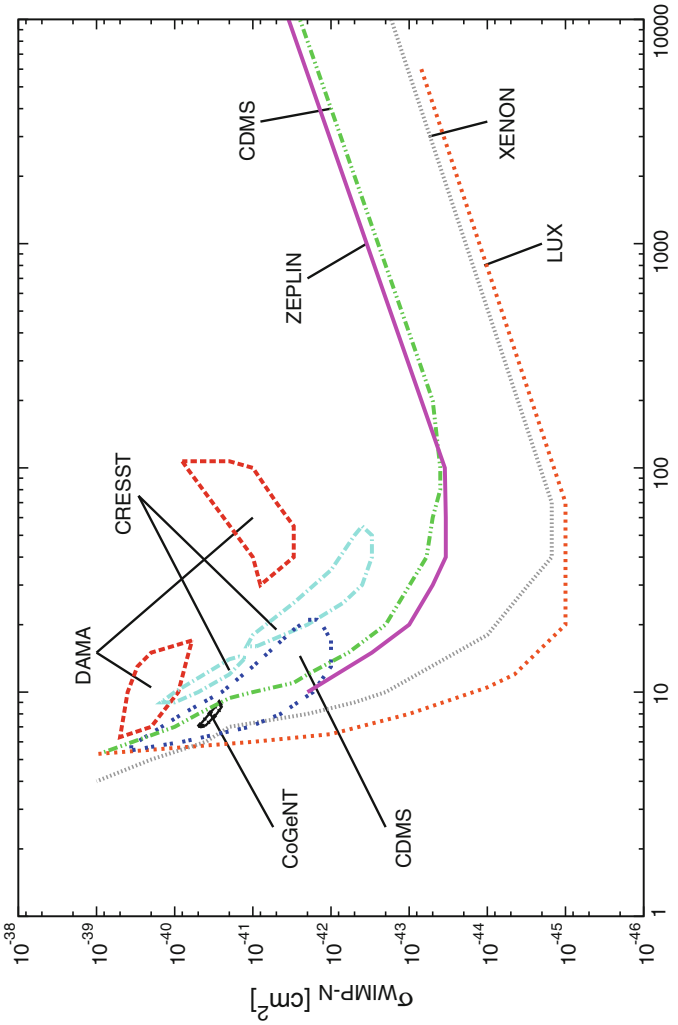

Fig. 9.3 Schematic summary of direct search for dark matter particles reporting the current limits from the experiments ZEPLIN (*magenta-solid line*), CDMS (*green-dashed double dotted line*), XENON (*gray-dotted line*), and LUX (*orange-dotted line*) and the possible dark matter signals from the experiments DAMA (*red-dashed closed curve*), CRESST (*light blue-dashed dotted closed curve*), CDMS (*blue-dotted closed curve*), and CoGeNT (*black-solid closed curve*). Dark matter candidates from the Minimal Supersymmetric Standard Model of particle physics are expected in the region $M_{WIMP} \sim 100$ GeV-1 TeV and $\sigma_{WIMP-N} \sim 10^{-49} - 10^{-45}$ cm^2, which is not yet explored. Possible dark matter signals have been found in the so-called low-mass WIMP region, but there is no agreement among different experiments

we exploit the relative motion of the Sun with respect to the Galaxy. The signal should be stronger in the direction of the motion of the Solar System, which could be distinguished from the background noise, since the latter is produced on Earth and should be isotropic.

Figure 9.3 shows the current status of the WIMP search. Most experiments provide limits on the WIMP detection in the mass-cross section plane. The shape of the constraints can be easily explained. At low masses, the sensitivity of the detector is limited by the detector energy threshold. For a WIMP mass in the range 10 GeV to 10 TeV, the expected nuclear recoil energies are usually in the range $1 - 100$ keV. At high masses, the sensitivity decreases because of the decreasing WIMP number flux, since ρ is fixed and $n = \rho/m$.

There are not only upper bounds but also statements of WIMP detection, which are however difficult to reconcile with the negative results of other experiments. The strongest claim comes from the DAMA/LIBRA collaboration: they have observed for several years an annual modulation in the event rate which would be consistent with the expected signal from WIMPs (see Fig. 9.4). More recently, CDMS, CRESST,

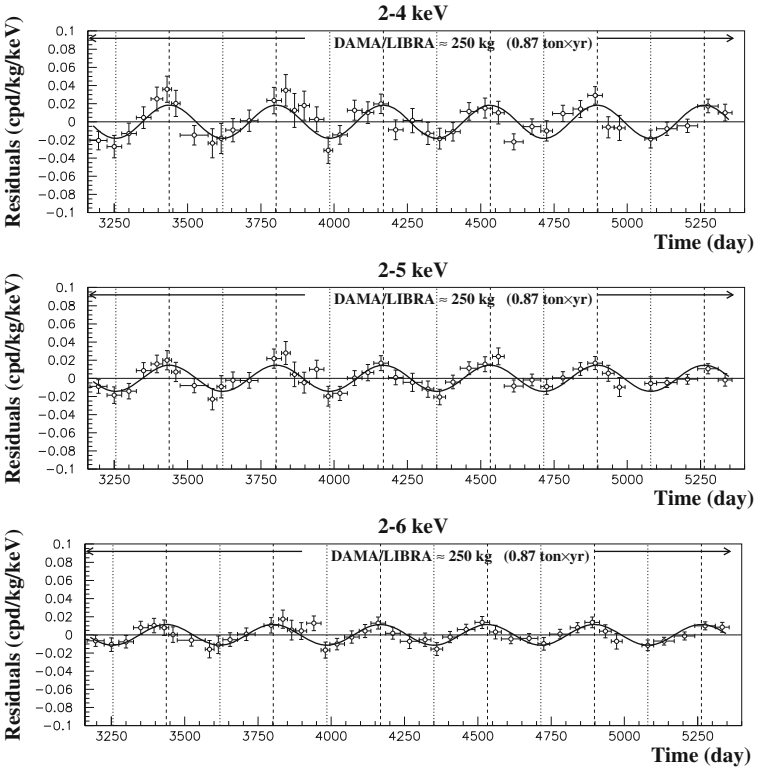

Fig. 9.4 Residual signal measured by DAMA/LIBRA $2-4$, $2-5$, and $2-6$ keV energy intervals as a function of time. From Bernabei (2010), under the terms of the creative commons attribution noncommercial license

and CoGeNT reported evidence of possible detections of WIMPs in their detectors, but there is no common consensus on the interpretation of these results, which seem also to be in conflict with the limits from other collaborations.

Direct search for axion dark matter proceeds in a completely different way. The idea is to observe the axion-photon transformation, $a \rightarrow \gamma$, in a strong magnetic field. The only running experiment is ADMX at the University of Washington Seattle. It is providing upper bounds on the $a\gamma\gamma$ coupling constant $g_{a\gamma\gamma}$ for μeV mass axions.

9.4 Indirect Search for Dark Matter Particles

Indirect quest for dark matter particles are performed by astronomical observations of possible products of their annihilation or decay. For instance, if there are equal densities of dark matter particles and antiparticles or if particles and antiparticles are the same, as expected in some scenarios, they may annihilate and produce γ-rays or e^+e^- and $\bar{p}p$ pairs. However, in the case of the so-called asymmetric dark matter, there is a dominant excess of particles over antiparticles (or vice versa) and these effects are absent.

Anyhow, an observation of an excess of γ-rays, antiprotons, positrons, or high energy neutrinos-antineutrinos in the cosmic ray background or from specific sources (e.g., the Sun or the Center of the Galaxy, where the dark matter density is expected to be higher) may be an indication of dark matter. Such a detection clearly requires a very good knowledge of the contribution from astrophysical processes and of the propagation of cosmic rays in the Galaxy, which is not usually the case. Indirect search for dark matter particles can be seen as complementary to direct detection experiments, since they may test different regions of the parameter space, where dark matter particles have different masses and coupling constants.

Some astronomical observations might have already registered dark matter signals, but systematics effects, in particular the contributions from astrophysical processes, are not really under control and there is no consensus on the interpretation of these data. In 2009, the PAMELA collaboration reported the observation of an excess of positrons in cosmic rays in the range $10-100$ GeV (see Fig. 9.5) (Adriani 2009). Their measurement was confirmed by other experiments. The observations by ATIC, FERMI/LAT, and H.E.S.S. also reported an excess of electrons and positrons in the range $100-1000$ GeV. However, the origin of these positrons is not yet clear. The required cross section to explain this excess is not consistent with that expected for thermal WIMPs. Some specific WIMP scenarios have been proposed in the literature to do it, but they seem now to be ruled out by the FERMI/LAT measurements of the flux of high energy photons. On the contrary, some astrophysical explanations, like positron production from pulsars of the Galaxy (Profumo 2011), appear more convincing.

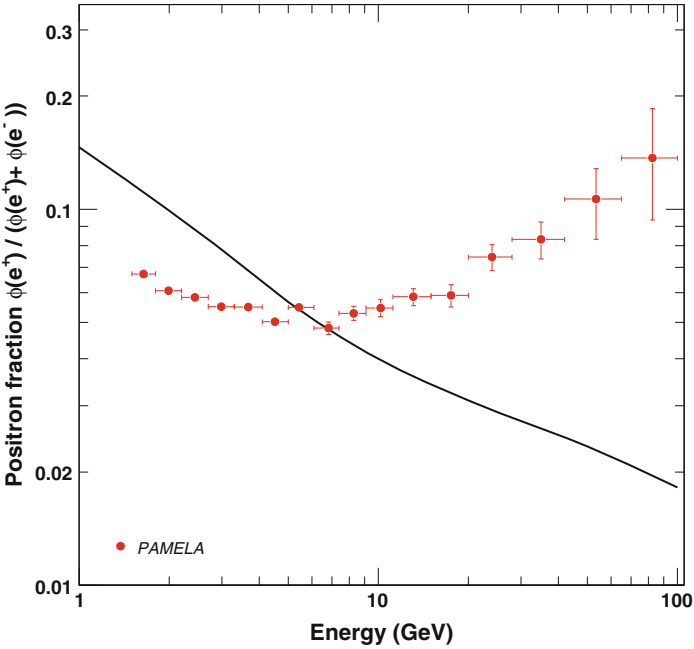

Fig. 9.5 The PAMELA positron fraction compared with a theoretical model (*black solid line*). Reprinted by permission from Macmillan Publishers Ltd: O. Adriani et al., Nature **458**, 607–609, copyright 2009. http://www.nature.com/

Problems

9.1 The dark matter energy density in the Solar System is estimated to be around 0.4 GeV/cm^3. Let us assume that dark matter consists of particles with a mass of 100 GeV, that they only interact via the weak nuclear force (exchange of W- and Z-bosons), and that their typical velocity is $v/c \sim 10^{-3}$.

(a) Estimate the dark matter particle flux (number of particles/cm^2/s) on Earth.
(b) Estimate the interaction rate of dark matter particles with a human being.
(c) How do the previous estimates change in the case of super-heavy dark matter particles with a mass of 10^{15} GeV?

References

R.J. Adler, P. Chen, D.I. Santiago, Gen. Rel. Grav. **33**, 2101 (2001) [gr-qc/0106080]
O. Adriani et al., PAMELA collaboration. Nature **458**, 607 (2009). arXiv:0810.4995 [astro-ph]
C. Afonso et al., EROS collaboration. Astron. Astrophys. **400**, 951 (2003) [astro-ph/0212176]
C. Alcock et al., MACHO collaboration. Astrophys. J. **542**, 281 (2000) [astro-ph/0001272]

C. Bambi, A.D. Dolgov, K. Freese, Nucl. Phys. B **763**, 91 (2007) [hep-ph/0606321]
L. Bergstrom, Rept. Prog. Phys. **63**, 793 (2000) [hep-ph/0002126]
R. Bernabei *et al.* [DAMA and LIBRA Collaborations], Eur. Phys. J. C **67**, 39 (2010). arXiv:1002.1028 [astro-ph.GA]
B.J. Carr, Lect. Notes Phys. **631**, 301 (2003) [astro-ph/0310838]
D. Clowe, A. Gonzalez, M. Markevitch, Astrophys. J. **604**, 596 (2004) [astro-ph/0312273]
K.C. Freeman, Astrophys. J. **160**, 811 (1970)
C. Lage, G.R. Farrar, arXiv:1406.6703 [astro-ph.GA]
D.N. Page, S.W. Hawking, Astrophys. J. **206**, 1 (1976)
P. Pani, A. Loeb, JCAP **1406**, 026 (2014). arXiv:1401.3025[astro-ph.CO]
S. Profumo, Central. Eur. J. Phys. **10**, 1 (2011). arXiv:0812.4457 [astro-ph]
G.G. Raffelt, in *Beyond the Desert 1997: Accelerator and Non-Accelerator Approaches* (Institute of Physics, London, 1998), pp. 808-815 [astro-ph/9707268]
M. Schumann. arXiv:1501.0120 [astro-ph.CO]
P. Tisserand et al., EROS-2 collaboration. Astron. Astrophys. **469**, 387 (2007) [astro-ph/0607207]